Nonlinear Dyn (2015) 81:1489–1510
DOI 10.1007/s11071-015-2083-4

ORIGINAL PAPER

Recursive terminal sliding mode control for hypersonic flight vehicle with sliding mode disturbance observer

Jianmin Wang · Yunjie Wu · Xiaomeng Dong

Received: 28 June 2014 / Accepted: 7 April 2015 / Published online: 3 May 2015

Abstract A recursive terminal sliding mode controller (RTSMC) based on sliding mode disturbance observer (SMDOB) is proposed for the longitudinal dynamics of a generic hypersonic flight vehicles (HFVs) in the presence of parametric uncertainties, measurement noises and external disturbances. First, a sliding mode tracking controller is presented by introducing recursive terminal sliding mode manifolds, in which each manifold will reach zero subsequently in finite time as well as the usual singularity problem will not occur. The RTSMC embraces advantages of both nonsingular terminal sliding mode control and high-order sliding mode control. Next, for the sake of enhancing the robustness of controller for uncertainties, a SMDOB is proposed to estimate and compensate the disturbances. Then, a composite controller that is composed of RTSMC and SMDOB is designed, and its stability is analyzed utilizing Lyapunov function method. Finally, numerical simulation is conducted for cruise flight condition of HFV. Simulation results show the expected control performance.

Keywords Recursive terminal sliding mode control · Sliding mode disturbance observer · Hypersonic flight vehicle · Finite time · Nonsingular terminal sliding mode

J. Wang (✉) · Y. Wu
State Key Laboratory of Virtual Reality Technology and Systems, Beihang University, Beijing 100191, China
e-mail: wjm123121@126.com

J. Wang · Y. Wu
School of Automation Science and Electrical Engineering, Beihang University, Beijing 100191, China

J. Wang · Y. Wu
Science and Technology on Aircraft Control Laboratory, Beihang University, Beijing 100191, China

X. Dong
Qian Xuesen Laboratory of Space Technology, CAST, Beijing 100094, China

1 Introduction

As a cost-effective and reliable space aircraft, HFVs have attracted more and more interests from civil and military due to its high-speed and prompt global responses. HFV is a class of aircrafts that flying in the near space which is 30–70 km from the ground. The atmospheric environment of near space is unstable, and the flight condition is complex. In addition, there are strong interactions in HFV between the engine dynamics and airframe. It is sensitive to any tiny uncertainty change due to the peculiar aerodynamic structure of HFV. Hence, it is a significant challenging task for modeling and control of HFV. The research of HFV started about 1960s, so fruitful results had been achieved up to date. In 2004, the flight tests of X43-A HFV were held successfully, which motivate the further research for modern control and application of HFV dynamic system. In the last decade, a variety of modern methods and techniques have been applied to the area of flight control design of HFV, and considerable research achievements have sprung up.

Aeropropulsive and aeroelastic of HFV were analyzed in detail in reference [1], which laid the foundation for establishing HFV model. Bolender and Doman [2,3] built a nonlinear model for the longitudinal dynamics of air-breathing HFV, which captured the complex interactions between the aerodynamics, propulsion system and structural dynamics, and its motion equations were derived using Lagrange's equations. In terms of nonlinear model, robust flight control systems were synthesized [4] that stability and performance robustness was estimated by Monte Carlo evaluation. And stochastic robust nonlinear dynamic inversion (NDI) control law was proposed for longitudinal motion of HFV containing 28 uncertain parameters [5]. For the sake of utilizing linear control method, feedback linearization model and control-oriented linearized model were derived in [6,7]. Xu [8] designed an adaptive sliding mode controller for longitudinal dynamics of input–output linearization model of HFV, where the input–output linearization model is proved to be an effective and extensively used model hereafter. Obaid proposed mini–max linear quadratic regulator (LQR) optimal controller and mini–max optimal linear quadratic Gaussian (LQG) controller by the virtue of mini–max linear quadratic theory for feedback linearization model of HFV, in which the optimal control minimizes the maximum value of the quadratic cost function and gives an optimal solution for the selected cost function [9–11]. The optimal controller can achieve good performance. However, the construction of Riccati equation parameter matrix in LQR is a difficulty work. Because of the peculiarity of many uncertainties for HFV model, sliding mode control is frequently adopted, which is not only robust to uncertainty but also easily designed.

The basic of sliding mode control is the designing of sliding mode surface. Different sliding surfaces can lead to various convergence performances. Integral sliding surface can eliminate the static error when the system is stable. Terminal sliding surface results in finite-time convergence for system states. Global sliding surface has global robustness due to its initial states on the sliding manifold. In reference [12], an integral-type sliding manifold is designed and then a nonfragile H_∞ controller based on that is investigated for a flexible air-breathing HFV. Taking into account adaptive sliding control, Burak putted forward a varying sliding surface with varying slopes and offsets, whose parameters were updated by solving state-dependent Riccati equations [13]. A robust sliding manifold-based adaptive sliding mode controller is presented in [14] for air-breathing HFV, where the system error dynamics can be driven onto the predefined sliding surface in finite time. Nevertheless, the system states do not always convergence to the equilibrium point in finite time once the system states are driven onto the sliding manifold. But the terminal sliding mode control can realize it.

For terminal sliding mode control, system states arrive at the sliding manifold from their initial conditions in finite time; then, the states slide along the sliding manifold to the equilibrium point in finite time. Therefore, the terminal sliding mode control is a kind of finite-time convergence control. So far, there are numerous research results about terminal sliding mode control, such as fast terminal sliding mode control design [15], continuous terminal sliding mode control [16], et al. Terminal sliding mode control usually has singularity problem which limits its application. For this, Yong Feng proposed nonsingular terminal sliding mode control and applied it to the rigid manipulators successfully [17]. Combining the above methods, Li [18] proposed an adaptive nonsingular fast terminal sliding mode control scheme for electromechanical actuator.

It is worth noting that HFV is a high-order nonlinear system. Hence, the low-order sliding mode controller for HFV has chattering phenomenon and slow converge speed. Albeit references [19,20] have presented high-order sliding mode control for HFV, their first sliding surfaces remain linear form, namely asymptotic convergence. Therefore, above both controllers do not converge in finite time. Aiming at the finite-time convergence problem, a recursive high-order terminal sliding mode control is proposed for HFV in this paper. The proposed scheme has robustness to uncertainty parameters.

In addition to the parameters uncertainty, there are external disturbance during the HFV flight. A small number of references consider external disturbance [19]. In this paper, a novel sliding mode disturbance observer (SMDOB) is presented, which can estimate the disturbance and further compensate it in the controller. As a result, the composite control in this paper is RTSMC+SMDOB, where RTSMC achieves command tracking control meanwhile eliminate chattering, and SMDOB estimates external disturbance and compensates it. The major contributions of this paper are as follows

(I) A novel recursive terminal sliding mode controller is proposed for hypersonic flight vehicles, which is the first time that the method is applied in hypersonic aircraft. The hypersonic flight vehicle is highly nonlinear, and the recursive sliding mode controller can meet its control requirements. The recursive terminal sliding mode controller is nonlinear controller, which is the superior than linear controller for nonlinear systems.

(II) The novel sliding mode control has merits of both nonsingular terminal sliding mode control (NTSMC) and high-order sliding mode control (HOSMC). The system states under this controller are finite-time convergent and have no singularity problem, and at the same time, the chattering problem existed in common sliding mode control is attenuated.

(III) A SMDOB is introduced for the external disturbance of HFV. The SMDOB is simple and not relay on the plant and has shorter estimated time than other methods. This disturbance observer cannot affect the controller designing and application, which is relatively independent in the whole system. The disturbance observer is as compensation part for the controller, by which the external disturbance is eliminated.

(IV) The engineering application of NTSMC and SMDOB is considered. In the process of designing, the methods are considered for implementation by hardware, not only in mathematical deduction. So these methods have a certain value of engineering application.

The remainder of the paper is organized as follows. Section 2 formulates the HFV model and control problem. Section 3 shows the design process of RTSMC and SMDOB in detail. The composite controller is presented in Sect. 4, and the stability analysis for controller is given at the same time. Numerical simulations are conducted in Sect. 5. Finally, Sect. 6 gives the conclusions.

2 Model and problem formulation

2.1 Hypersonic flight vehicle model

The model of longitudinal dynamics for a generic HFV is developed by NASA Langley Research Center, which consists of differential equations described by velocity, altitude, angle of attack, flight path angle and pitch rate [8,21]. The motion equations are as follows:

$$\begin{cases} \dot{V} = \frac{T\cos\alpha - D}{m} - \frac{\mu\sin\gamma}{r^2} \\ \dot{h} = V\sin\gamma \\ \dot{\gamma} = \frac{L+T\sin\alpha}{mV} - \frac{(\mu - V^2 r)\cos\gamma}{Vr^2} \\ \dot{\alpha} = q - \dot{\gamma} \\ \dot{q} = \frac{M_{yy}}{I_{yy}} \end{cases} \tag{1}$$

where V, h, γ, α, q are velocity, altitude, flight path angle, angle of attack and pitch rate of HFV, respectively; m is mass and I_{yy} is moment of inertia of the aircraft; L, D, T, M_{yy} are lift, drag, thrust, pitching moment, respectively, that acting on the aircraft and r is radial distance from Earth's center. The expression details of L, D, T, M_{yy}, r are, respectively, as follows

$$L = \frac{1}{2}\rho V^2 \mathrm{S}C_L \tag{2}$$

$$D = \frac{1}{2}\rho V^2 S C_D \tag{3}$$

$$T = \frac{1}{2}\rho V^2 S C_T \tag{4}$$

$$M_{yy} = \frac{1}{2}\rho V^2 S\bar{c}\left[C_M(\alpha) + C_M(\alpha,\delta_e) + C_M(\alpha,q)\right] \tag{5}$$

$$r = h + R_E \tag{6}$$

where $\rho, S, \bar{c}, R_E$ denote density of air, reference area, mean aerodynamic chord and radius of the Earth, respectively; δ_e is the elevator deflection angle; $C_L, C_D, C_T, C_M(\alpha), C_M(\alpha,\delta_e), C_M(\alpha,q)$ are relevant aerodynamic coefficient parameters, respectively, as

$$C_L = 0.6203\alpha \tag{7}$$

$$C_D = 0.6450\alpha^2 + 0.0043378\alpha + 0.003772 \tag{8}$$

$$C_T = \begin{cases} 0.02576\beta, & \beta < 1 \\ 0.0224 + 0.00336\beta, & \beta > 1 \end{cases} \tag{9}$$

$$C_M(\alpha) = -0.035\alpha^2 + 0.036617(1 + \Delta C_{M\alpha})\alpha + 5.3261 \times 10^{-6} \tag{10}$$

$$C_M(\alpha,q) = \frac{\bar{c}q}{2V}\left(-6.796\alpha^2 + 0.3015\alpha - 0.2289\right) \tag{11}$$

$$C_M(\alpha,\delta_e) = c_e\left(\delta_e + d_2(t) - \alpha\right) \tag{12}$$

where $d_2(t)$ means the external disturbance reflected on the elevator.

A second-order system is used to represent the engine dynamics as

$$\ddot{\beta} = -2\zeta\omega_n\dot{\beta} - \omega_n^2\beta + \omega_n^2\left(\beta_c + d_1(t)\right) \tag{13}$$

where β and β_c are throttle setting and throttle setting command, respectively; ξ is damping ratio and ω_n is natural frequency; $d_1(t)$ is the external disturbance on behalf of torques and generalized elastic forces.

In order to certify the robustness and immunity of the proposed controller, some certain parameter uncertainties are added in the HFV model that

$$\begin{cases} m = m_0\left(1+\Delta m\right) \\ I_{yy} = I_0\left(1+\Delta I\right) \\ S = S_0\left(1+\Delta S\right) \\ \bar{c} = \bar{c}_0\left(1+\Delta\bar{c}\right) \\ \rho = \rho_0\left(1+\Delta\rho\right) \\ c_e = c_{e0}(1+\Delta c_e) \\ C_{M\alpha} = C_{M\alpha 0}(1+\Delta C_{M\alpha}) \end{cases} \tag{14}$$

where $(\bullet_0)$ represents the nominal value of the parameter $(\bullet)$ and $(\Delta\bullet)$ denotes the parameter uncertainties.

Assumption 1 The external disturbance $d_i(t)$ and its first time derivative are assumed to be upper bounded [21,22], i.e., $|d_i(t)| \le g_i$, $\left|\dot{d}_i(t)\right| \le \bar{g}_i$, here g_i and $\bar{g}_i$ are known positive constants for $i = 1, 2$.

Assumption 2 The parameter uncertainties in Eq. (14) are assumed to be bounded. And they satisfy the following conditions:

$$|\Delta m| \le \Delta m^*, |\Delta I| \le \Delta I^*, |\Delta S| \le \Delta S^*, |\Delta\bar{c}| \le \Delta\bar{c}^*,$$
$$|\Delta\rho| \le \Delta\rho^*, |\Delta c_e| \le \Delta c_e^*, |\Delta C_{M\alpha}| \le \Delta C_{M\alpha}^*$$

where $\Delta m^*, \Delta I^*, \Delta S^*, \Delta\bar{c}^*, \Delta\rho^*, \Delta c_e^*, \Delta C_{M\alpha}^*$ are all positive real constants.

Remark 1 According to model (1), velocity V and altitude h are regarded as output variables, while the input variables are selected as engine throttle setting command β_c and elevator deflection δ_e. The control objective is designing a suitable controller such that the velocity V and altitude h track the command V_d and h_d in finite time in the presence of uncertainty, noises and disturbance, respectively.

2.2 Input–output linearization

The model of HFV in Eq. (1) is highly nonlinear and strong coupling. For the sake of designing control law expediently, input–output linearization method needs to be applied to linearize the model. In terms of Remark 1, the linearization target is that the linearized results can apparently express the relationship between output variables (V, h) and input variables (β_c, δ_e).

In line with the nonlinear system theory and taking advantage of tools for Lie derivative, it is concluded that input variables (β_c, δ_e) can appear in the motion equations by differentiating V three times and h four times [8], respectively. So the relative degree of the HFV nonlinear system is $r = 3 + 4 = 7$. Due to the order of system in Eq. (1) is five, a second-order engine dynamics system is introduced. Therefore, the order of whole system is seven, i.e., $n = 5 + 2 = 7$. In terms of $r = n$, the closed-loop system has no zero dynamics [23] and the nonlinear longitudinal model can be linearized completely [5]. The linearization process is as follows

$$\begin{cases} \dot{V} = f_V(\mathbf{x}) \\ \ddot{V} = \boldsymbol{\Omega}_1\dot{\mathbf{x}}/m \\ \dddot{V} = (\boldsymbol{\Omega}_1\ddot{\mathbf{x}} + \dot{\mathbf{x}}^{\mathrm{T}}\boldsymbol{\Omega}_2\dot{\mathbf{x}})/m \end{cases} \tag{15}$$

$$\begin{cases} \dot{h} = \dot{V}\sin\gamma + V\dot{\gamma}\cos\gamma \\ \ddot{h} = \ddot{V}\sin\gamma + 2\dot{V}\dot{\gamma}\cos\gamma - V\dot{\gamma}^2\sin\gamma + V\ddot{\gamma}\cos\gamma \\ h^{(4)} = \dddot{V}\sin\gamma + 3\ddot{V}\dot{\gamma}\cos\gamma - 3\dot{V}\dot{\gamma}^2\sin\gamma + 3\dot{V}\ddot{\gamma}\cos\gamma \\ \qquad - 3V\dot{\gamma}\ddot{\gamma}\sin\gamma - V\dot{\gamma}^3\cos\gamma + V\dddot{\gamma}\cos\gamma \end{cases} \tag{16}$$

$$\dot{\gamma} = f_h(\mathbf{x}),\ \ddot{\gamma} = \boldsymbol{\Pi}_1\dot{\mathbf{x}},\ \dddot{\gamma} = \boldsymbol{\Pi}_1\ddot{\mathbf{x}} + \dot{\mathbf{x}}^{\mathrm{T}}\boldsymbol{\Pi}_2\dot{\mathbf{x}} \tag{17}$$

where $\mathbf{x} = [\,V\ \gamma\ \alpha\ \beta\ h\,]^{\mathrm{T}}$ is the state vector, $\boldsymbol{\Omega}_1, \boldsymbol{\Omega}_2$, $\boldsymbol{\Pi}_1, \boldsymbol{\Pi}_2$ are the system equations' first-order and second-order partial derivatives regarding to state variables, respectively, whose detailed expressions are shown in "Appendix 1."

The expressions of $\ddot{\alpha}$ and $\ddot{\beta}$ can be written two parts as

$$\begin{aligned} \ddot{\alpha} &= \ddot{\alpha}_0 + \frac{\rho V^2 S\bar{c}c_e}{2I_{yy}}\left(\delta_e + d_2(t)\right) \\ \ddot{\beta} &= \ddot{\beta}_0 + \omega_n^2\left(\beta_c + d_1(t)\right) \end{aligned} \tag{18}$$

where

$$\ddot{\alpha}_0 = \frac{1}{2I_{yy}}\rho V^2 S\bar{c}\left[C_M(\alpha) + C_M(\alpha, q) - c_e\alpha\right] - \dddot{\gamma}$$
$$\ddot{\beta}_0 = -2\xi\omega_n\dot{\beta} - \omega_n^2\beta$$

Given $\ddot{\mathbf{x}}_0 = [\,\ddot{V}\ \dddot{\gamma}\ \ddot{\alpha}_0\ \ddot{\beta}_0\ \ddot{h}\,]^{\mathrm{T}}$, then

$$\begin{cases} \dddot{V} = F_V + b_{11}\left(\beta_c + d_1(t)\right) + b_{12}\left(\delta_e + d_2(t)\right) \\ h^{(4)} = F_h + b_{21}\left(\beta_c + d_1(t)\right) + b_{22}\left(\delta_e + d_2(t)\right) \end{cases} \tag{19}$$

where

$$F_V = \frac{\left(\boldsymbol{\Omega}_1 \ddot{\boldsymbol{x}}_0 + \dot{\boldsymbol{x}}^{\mathrm{T}} \boldsymbol{\Omega}_2 \dot{\boldsymbol{x}}\right)}{m}$$

$$\begin{aligned} F_h = {} & 3\ddot{V}\dot{\gamma}\cos\gamma - 3\dot{V}\dot{\gamma}^2\sin\gamma + 3\dot{V}\ddot{\gamma}\cos\gamma \\ & - 3V\dot{\gamma}\ddot{\gamma}\sin\gamma - V\dot{\gamma}^3\cos\gamma + F_V\sin\gamma \\ & + V\cos\gamma\left(\boldsymbol{\Pi}_1\ddot{\boldsymbol{x}}_0 + \dot{\boldsymbol{x}}^{\mathrm{T}}\boldsymbol{\Pi}_2\dot{\boldsymbol{x}}\right) \end{aligned}$$

$$b_{11} = \left(\frac{\rho V^2 S c_\beta \omega_n^2}{2m}\right)\cos\alpha$$

$$b_{12} = -\left(\frac{c_e \rho V^2 S\bar{c}}{2mI_{yy}}\right)(T\sin\alpha + D_\alpha)$$

$$b_{21} = \left(\frac{\rho V^2 S c_\beta \omega_n^2}{2m}\right)\sin(\alpha+\gamma)$$

$$\begin{aligned} b_{22} = {} & \left(\frac{c_e \rho V^2 S\bar{c}}{2mI_{yy}}\right)\left[T\cos(\alpha+\gamma)\right. \\ & \left. + L_\alpha\cos\gamma - D_\alpha\sin\gamma\right] \end{aligned}$$

$$c_\beta = \frac{\partial C_T}{\partial\beta},\ D_\alpha = \frac{\partial D}{\partial\alpha},\ L_\alpha = \frac{\partial L}{\partial\alpha}$$

Then, Eq. (19) can be rewritten as

$$\begin{bmatrix} \ddot{V} \\ h^{(4)} \end{bmatrix} = \begin{bmatrix} F_V \\ F_h \end{bmatrix} + \mathbf{B}\begin{bmatrix} \beta_c \\ \delta_e \end{bmatrix} + \mathbf{B}\begin{bmatrix} d_1(t) \\ d_2(t) \end{bmatrix} \tag{20}$$

where $\mathbf{B} = \begin{bmatrix} b_{11} & b_{12} \\ b_{21} & b_{22} \end{bmatrix}$.

Assumption 3 The matrix $\mathbf{B}$ is assumed to be invertible.

Remark 2 For the input–output combination, the matrix $\mathbf{B}$ is nonsingular for the entire flight envelope except on a vertical flight path [5]. Hence, the Assumption 3 is reasonable to be assumed. When the flight condition is near the singularity, the measures taken are shown in "Appendix 2."

Remark 3 The nonlinear system in Eq. (1) can be expressed as affine nonlinear system of form

$$\begin{aligned} \dot{\boldsymbol{x}}(t) &= \boldsymbol{f}(\boldsymbol{x}) + \sum_{k=1}^{m} \boldsymbol{g}_k(\boldsymbol{x})u_k \\ y_i &= h_i(\mathbf{x}), \quad i = 1, 2, \ldots, m \end{aligned}$$

where $\boldsymbol{f}, \boldsymbol{g}, \boldsymbol{h}$ are smooth functions in $\boldsymbol{R}^n$. In terms of above contents, relative degree of the system, $r = n$, the order of the system, there is no zero dynamics. Therefore, the control input $u = \left[\beta_c\ \delta_e\right]^{\mathrm{T}}$ in linearized system (20) is affine control input.

Remark 4 Given $x_1 = v, x_2 = \dot{v}, x_3 = \ddot{v}$, the velocity subsystem is changed to the form of state space without considering the external disturbance as

$$\begin{bmatrix} \dot{x}_1 \\ \dot{x}_2 \\ \dot{x}_3 \end{bmatrix} = \begin{bmatrix} 0 & 1 & 0 \\ 0 & 0 & 1 \\ a_{11} & a_{12} & a_{13} \end{bmatrix}\begin{bmatrix} x_1 \\ x_2 \\ x_3 \end{bmatrix} + \begin{bmatrix} 0 & 0 \\ 0 & 0 \\ b_{11} & b_{12} \end{bmatrix}\begin{bmatrix} \beta_c \\ \delta_e \end{bmatrix}$$

$$y = \begin{bmatrix} 1\ 0\ 0 \end{bmatrix}\begin{bmatrix} x_1 \\ x_2 \\ x_3 \end{bmatrix} + \begin{bmatrix} 0\ 0 \end{bmatrix}\begin{bmatrix} \beta_c \\ \delta_e \end{bmatrix}$$

where a_{1i} is related to F_V and $a_{1i} \neq 0, i = 1, 2, 3$. The system matrixes are, respectively,

$$\boldsymbol{A} = \begin{bmatrix} 0 & 1 & 0 \\ 0 & 0 & 1 \\ a_{11} & a_{12} & a_{13} \end{bmatrix},\quad \boldsymbol{B} = \begin{bmatrix} 0 & 0 \\ 0 & 0 \\ b_{11} & b_{12} \end{bmatrix},$$

$$\boldsymbol{C} = \begin{bmatrix} 1\ 0\ 0 \end{bmatrix},\quad \boldsymbol{D} = \begin{bmatrix} 0\ 0 \end{bmatrix}.$$

According to the **output controllability criterion** [24], the output V is controllable.

Similarly, the output variable h is also controllable.

In one word, the input–output linearized model is controllable, and the system can be stable if the controller is appropriate.

3 Controller and observer design

In this section, a recursive terminal sliding mode controller is firstly designed to track the reference command, and then, a sliding mode disturbance observer is presented for compensating the external disturbance.

3.1 Tracking controller design

Terminal sliding mode control usually has the singularity problem. An approximately terminal sliding mode control can be introduced according to the sliding mode twisting algorithm, which can avoid the singularity problem.

Lemma 1 [25,26] *Define a derivative–integral terminal sliding function for a second-order system as*

$$s = \dot{e} + \beta e + \alpha e_I \tag{21}$$

where $\alpha, \beta > 0, \dot{e}_I(t) + T_s e_I(t) = sign\,(e(t))$ *with the system tracking error* $e(t)$.

When the initial condition is chosen as $e_I(0) = -(\dot{e}(0) + \beta e(0))/\alpha$, then the system tracking error e will converge to zero in finite time, i.e., the convergence time t_{reach} has an upper bound.

Proof Substituting the initial condition into Eq. (21) yields $s = 0$. In other words, the system tracking error trajectory is on the sliding mode manifold that

$$s = \dot{e} + \beta e + \alpha e_I = 0 \tag{22}$$

Define

$$z = -\alpha e_I \tag{23}$$

Then

$$\dot{e} = z - \beta e \tag{24}$$

According to [25], an arbitrary absolutely continuous function $V(e, z)$ can be found satisfying

$$\dot{e} \cdot \frac{\partial V}{\partial e} - \alpha \cdot \frac{\partial V}{\partial z} = k \cdot V^{1/2} \tag{25}$$

Choose $s(e, z)$ and $m(e, z)$, respectively, as

$$s(e, z) = 2\alpha\,|e| - \beta e z + z^2 > 0 \quad \text{for } e^2 + z^2 \neq 0 \tag{26}$$

$$m(e, z) = \frac{1}{\sqrt{g-1}} arc\tan\frac{\beta g e - 2z}{2\sqrt{g-1}z} \tag{27}$$

where $g = 8\alpha/\beta^2$.

Then, the Lyapunov function candidate $V(e, z)$ can be written as

$$V(e, z) = \frac{k^2}{4}\left(-e_I + k_0 e^{m(e,z)}\sqrt{s(e, z)}\right)^2 \tag{28}$$

where $k_0 > -z \cdot \left(\alpha e^{m(e,z)}\sqrt{s(e, z)}\right)^{-1}$.

In accordance with Theorem 1 in [25], the reaching time has an upper bound, i.e.,

$$t_{\text{reach}} \leq 2k_{\min}^{-1} \max\left\{\sqrt{V\left(e(0), z(0)\right)}\right\} \tag{29}$$

where

$$k_{\min} = \frac{\beta}{\sqrt{8}} \min_{g \in \{g^-, g^+\}} \left\{ g\bar{k} - \sqrt{g} e^{\arctan\left(\frac{-1}{\sqrt{g-1}}\right)/\sqrt{g-1}} \right\},$$
$$\bar{k} > 0.$$

Therefore, the system tracking error e will converge to zero in finite time t_{reach}. The proof is completed. □

Remark 5 The above Lemma is generated in terms of sliding mode twisting algorithm. In other words, the tracking error e and its integration state e_I converge to zero along sliding mode twisting trajectory in finite time. The merit is that fewer nonlinear operations are employed.

Theorem 1 *Consider the HFV model (1) and its linearization form (20) based on Assumption 3 and Remark 3, the system output variables V and h can track the reference command V_d and h_d in finite time, respectively, if the affine controller is chosen as*

$$u = \mathbf{B}^{-1}\begin{bmatrix} -\Phi_1 - F_V + \dddot{V}_d - k_1\,|s_1|^{\gamma_1}\,sgn(s_1) \\ -\Phi_2 - F_h + h_d^{(4)} - k_2\,|s_2|^{\gamma_2}\,sgn(s_2) \end{bmatrix} \tag{30}$$

where $k_1 > 0, k_2 > 0, 0 < \gamma_1 < 1, 0 < \gamma_2 < 1$. The recursive sliding mode manifolds, respectively, as

$$e_{11} = \dot{e}_{01} + \beta_{11} e_{01} + \alpha_{11} e_{I11} \tag{31a}$$
$$e_{21} = \dot{e}_{11} + \beta_{21} e_{11} + \alpha_{21} e_{I21} \tag{31b}$$
$$s_1 = e_{21} \tag{31c}$$

$$e_{02} = \dot{e}_2 + \lambda_2 e_2 \tag{32a}$$
$$e_{12} = \dot{e}_{02} + \beta_{12} e_{02} + \alpha_{12} e_{I12} \tag{32b}$$
$$e_{22} = \dot{e}_{12} + \beta_{22} e_{12} + \alpha_{22} e_{I22} \tag{32c}$$
$$s_2 = e_{22} \tag{32d}$$

where $e_{01} = V - V_d, e_2 = h - h_d$ are tracking errors, λ_2 is strictly positive constant, $\dot{e}_{I1i} + T_s e_{I1i} = sat\left(e_{0i}/\mu_{1i}\right), \dot{e}_{I2i} + T_s e_{I2i} = sat\left(e_{1i}/\mu_{2i}\right), T_s > 0, \mu_{1i}, \mu_{2i} > 0$ for $i = 1, 2$.

Proof Taking time derivative for Eq. (31) yields

$$\begin{aligned} \dot{e}_{11} &= \ddot{e}_{01} + \beta_{11}\dot{e}_{01} + \alpha_{11}\dot{e}_{I11} \\ \ddot{e}_{11} &= e_{01} + \beta_{11}\ddot{e}_{01} + \alpha_{11}\ddot{e}_{I11} \\ \dot{e}_{21} &= \ddot{e}_{11} + \beta_{21}\dot{e}_{11} + \alpha_{21}\dot{e}_{I21} \end{aligned} \tag{33}$$

$$\dot{s}_1 = \dot{e}_{21} = \dddot{e}_{01} + \beta_{11}\ddot{e}_{01} + \alpha_{11}\ddot{e}_{I11} + \beta_{21}\dot{e}_{11} + \alpha_{21}\dot{e}_{I21} \tag{34}$$

where

$$\ddot{e}_{I11} = M_{s1} - T_s \dot{e}_{I11}$$
$$M_{s1} = \begin{cases} \dot{e}_{01}/\mu_{11}, & |e_{01}/\mu_{11}| \leq 1 \\ 0, & otherwise \end{cases}.$$

Due to $\dddot{e}_{01} = \dddot{V} - \dddot{V}_d$, Eq. (34) is changed as

$$\dot{s}_1 = \dddot{V} - \dddot{V}_d + \Phi_1 \tag{35}$$

where

$$\Phi_1 = \beta_{11}\ddot{e}_{01} + \alpha_{11}\ddot{e}_{I11} + \beta_{21}\dot{e}_{11} + \alpha_{21}\dot{e}_{I21}$$

Similarly, taking first time derivative for Eq. (32) yields

$$\begin{aligned}
\dot{e}_{02} &= \ddot{e}_2 + \lambda_2 \dot{e}_2 \\
\ddot{e}_{02} &= \dddot{e}_2 + \lambda_2 \ddot{e}_2 \\
\dddot{e}_{02} &= e_2^{(4)} + \lambda_2 \dddot{e}_2 \qquad (36) \\
\dot{e}_{12} &= \ddot{e}_{02} + \beta_{12} \dot{e}_{02} + \alpha_{12} \dot{e}_{I12} \\
\ddot{e}_{12} &= e_2^{(4)} + \lambda_2 \dddot{e}_2 + \beta_{12} \ddot{e}_{02} + \alpha_{12} \ddot{e}_{I12} \\
\dot{e}_{22} &= \ddot{e}_{12} + \beta_{22} \dot{e}_{12} + \alpha_{22} \dot{e}_{I22} \qquad (37)
\end{aligned}$$

where

$$\begin{aligned}
\ddot{e}_{I12} &= M_{s2} - T_s \dot{e}_{I12} \\
M_{s2} &= \begin{cases} \dot{e}_{02}/\mu_{12}, & |e_{02}/\mu_{12}| \le 1 \\ 0, & \text{otherwise} \end{cases} . \\
\dot{s}_2 &= \dot{e}_{22} = e_2^{(4)} + \lambda_2 \dddot{e}_2 + \beta_{12} (\dddot{e}_2 + \lambda_2 \ddot{e}_2) \\
&\quad + \alpha_{12} \ddot{e}_{I12} + \beta_{22} \dot{e}_{12} + \alpha_{22} \dot{e}_{I22} \qquad (38)
\end{aligned}$$

Substituting $e_2^{(4)} = h^{(4)} - h_d^{(4)}$ into Eq. (38), yields

$$\dot{s}_2 = h^{(4)} - h_d^{(4)} + \Phi_2 \qquad (39)$$

where

$$\begin{aligned}
\Phi_2 &= \lambda_2 \dddot{e}_2 + \beta_{12} (\dddot{e}_2 + \lambda_2 \ddot{e}_2) + \alpha_{12} \ddot{e}_{I12} \\
&\quad + \beta_{22} \dot{e}_{12} + \alpha_{22} \dot{e}_{I22}
\end{aligned}$$

Then, Eq. (35) and Eq. (39) are expressed together as

$$\begin{bmatrix} \dot{s}_1 \\ \dot{s}_2 \end{bmatrix} = \begin{bmatrix} \dddot{V} \\ h^{(4)} \end{bmatrix} - \begin{bmatrix} \dddot{V}_d \\ h_d^{(4)} \end{bmatrix} + \begin{bmatrix} \Phi_1 \\ \Phi_2 \end{bmatrix} \qquad (40)$$

Substituting Eq. (20) in the absence of external disturbance into Eq. (40) acquires

$$\begin{bmatrix} \dot{s}_1 \\ \dot{s}_2 \end{bmatrix} = \begin{bmatrix} F_V \\ F_h \end{bmatrix} - \begin{bmatrix} \dddot{V}_d \\ h_d^{(4)} \end{bmatrix} + \begin{bmatrix} \Phi_1 \\ \Phi_2 \end{bmatrix} + \mathbf{B} \cdot u \qquad (41)$$

Choose a Lyapunov function candidate as

$$L_y = \frac{1}{2} s^{\mathrm{T}} s \qquad (42)$$

where $s = \begin{bmatrix} s_1 & s_2 \end{bmatrix}^{\mathrm{T}}$.

The derivative of L_y satisfies

$$\dot{L}_y = s^{\mathrm{T}} \dot{s} = s^{\mathrm{T}} \left(\begin{bmatrix} F_V \\ F_h \end{bmatrix} - \begin{bmatrix} \dddot{V}_d \\ h_d^{(4)} \end{bmatrix} + \begin{bmatrix} \Phi_1 \\ \Phi_2 \end{bmatrix} + \mathbf{B} \cdot u \right) \qquad (43)$$

Substituting Eq. (30) into Eq. (43) acquires

$$\begin{aligned}
\dot{L}_y &= s^{\mathrm{T}} \begin{bmatrix} -k_1 |s_1|^{\gamma_1} \operatorname{sgn}(s_1) \\ -k_2 |s_2|^{\gamma_2} \operatorname{sgn}(s_2) \end{bmatrix} \\
&= -k_1 |s_1|^{\gamma_1 + 1} - k_2 |s_2|^{\gamma_2 + 1} \le 0 \qquad (44)
\end{aligned}$$

Hence, the system states arrive at sliding manifolds s_1 and s_2 in finite time, i.e., the reaching time is $t_{s_i} = |s_i(0)|^{1-\gamma_i} / (k_i (1 - \gamma_i))$ for $i = 1, 2$. When system states slides along the sliding manifolds, then it has $s_i = e_{2i} = 0$ for $i = 1, 2$. In terms of Eqs. (31b) and (32c), the results are acquired

$$e_{2i} = 0 = \dot{e}_{1i} + \beta_{2i} e_{1i} + \alpha_{2i} e_{I2i}, \quad i = 1, 2 \qquad (45)$$

According to Lemma 1, e_{1i} will converge to zero in finite time, namely the convergence time $t_{\text{reach}}^{e_{1i}}$ has an upper bound. Then, substituting $e_{1i} = 0$ into Eqs. (31a) and (32b) yields

$$\dot{e}_{0i} + \beta_{1i} e_{0i} + \alpha_{1i} e_{I1i} = 0, \quad i = 1, 2 \qquad (46)$$

Similarly, e_{0i} will also converge to zero in finite time, and the convergence time $t_{\text{reach}}^{e_{0i}}$ has an upper bound. Then consider Eq. (32a) in accordance with $e_{02} = 0$ that

$$\dot{e}_2 + \lambda_2 e_2 = 0 \qquad (47)$$

It is worth noting that Eq. (47) is asymptotic convergence. Define an arbitrary small neighborhood for e_2, i.e., $Z_{e_2} \in [-\delta, +\delta], \delta > 0$. Once the altitude tracking error converging to the neighborhood, it is regarded that the altitude h had tracked the command h_d. Then, the convergence time is

$$t_{e_2} = \frac{1}{\lambda_2} (\ln (e_2(0)) - \ln \delta) \qquad (48)$$

Therefore, the convergence time of the velocity tracking error e_{01} is

$$t_1 = t_{s_1} + t_{\text{reach}}^{e_{11}} + t_{\text{reach}}^{e_{01}} \qquad (49)$$

For the altitude subsystem, the arriving time to the neighborhood Z_{e_2} is

$$t_2 = t_{s_2} + t_{\text{reach}}^{e_{12}} + t_{\text{reach}}^{e_{02}} + t_{e_2} \qquad (50)$$

In brief, the system output variables V and h can track the reference command V_d and h_d, respectively, in finite time. This completes the proof. □

Remark 6 For the velocity subsystem, there are three layers for sliding mode manifolds and four layers for the altitude subsystem. In each subsystem, these sliding manifolds are recursive. The last-layer sliding manifold is first arrived, and at this time, the finite-time arriving condition for the second layer is met. After a period of time, the second-layer sliding manifold is also arrived. In this order, each sliding manifold is arrived successively. Finally, the system tracking error can converge to zero in limited time.

Remark 7 Due to no singular terms appearing on Theorem 1 and all derivative terms are well defined, there is no singularity problem that usually arising in terminal sliding mode control.

3.2 Sliding mode disturbance observer design

The above proposed controller has robust for parameter uncertainties. However, for external disturbances, an additional disturbance observer is needed to compensate its influence to controller. In this section, a sliding mode disturbance observer is presented for the bounded external disturbance. Before designing, the equation in the presence of external disturbance is displayed. Substituting Eq. (20) into Eq. (40) acquires

$$\dot{s} = \mathbf{\Psi} + \hat{\mathbf{U}} + \hat{\mathbf{D}} \tag{51}$$

where

$$\dot{s} = \begin{bmatrix} \dot{s}_1 \\ \dot{s}_2 \end{bmatrix}, \mathbf{\Psi} = \begin{bmatrix} F_V - \dddot{V}_d + \Phi_1 \\ F_h - h_d^{(4)} + \Phi_2 \end{bmatrix},$$
$$\hat{\mathbf{U}} = \mathbf{B} \cdot u, \hat{\mathbf{D}} = \mathbf{B} \cdot \begin{bmatrix} d_1(t) \\ d_2(t) \end{bmatrix}.$$

Lemma 2 [27] *Assume an perturbed nonlinear differential equation*

$$\dot{x} + \omega_1 |x|^{1/2} sgn(x) + \omega_2 P(x) = \xi(t) \tag{52}$$

where $\dot{P}(x) + T_s P(x) = sgn(x)$, $\left|\dot{\xi}(t)\right| \le D$, D *is an positive constant.*

If $\omega_1 = 1.5\sqrt{D}$, $\omega_2 = 1.1D$, *then the solution* $x(t)$ *of above equation and its first time derivative* $\dot{x}(t)$ *converge to zero in finite time, i.e.,*

$$T_r \le \frac{7.6x(0)}{\omega_2 - D} \tag{53}$$

where T_r *is the convergence time and* $x(0)$ *is the initial value of* $x(t)$ *at* $t = 0$.

Theorem 2 *Consider the linearization system* (20) *with bounded external disturbance* $d_i(t)$, *which satisfy Assumption* 1. *Then, the external disturbance* $d_i(t)$ *can be exactly estimated in finite time, namely*

$$T_{ri} \le \frac{7.6\sigma_i(0)}{\omega_{2i} - \tilde{g}_i} \tag{54}$$

If the auxiliary sliding mode control variables are chosen as

$$v_i = \omega_{1i} |\sigma_i|^{1/2} sgn(\sigma_i) + \omega_{2i} P(\sigma_i) \tag{55}$$

where $\dot{P}(\sigma_i) + T_s P(\sigma_i) = sgn(\sigma_i)$, $\omega_{1i} = 1.5\sqrt{\tilde{g}_i}$, $\omega_{2i} = 1.1\tilde{g}_i$ *for* $i = 1, 2$.

Proof Choose an auxiliary sliding mode variable as

$$\sigma_i = s_i + z_i \tag{56}$$

$$\dot{z}_i = -\Psi_i - \bar{U}_i - v_i \tag{57}$$

where $i = 1, 2$.

According to Eqs. (56) and (57), Eq. (51) can be rewritten as

$$\dot{s}_i = \Psi_i + \bar{U}_i + \bar{D}_i, \quad i = 1, 2 \tag{58}$$

The σ_i dynamics is derived in terms of Eq. (58) as

$$\begin{aligned} \dot{\sigma}_i = \dot{s}_i + \dot{z}_i &= \Psi_i + \bar{U}_i + \bar{D}_i \\ &+ \left(-\Psi_i - \bar{U}_i - v_i\right) = \bar{D}_i - v_i \end{aligned} \tag{59}$$

Substituting Eq. (55) into Eq. (59), then the σ_i dynamics is changed as

$$\dot{\sigma}_i = \bar{D}_i - \omega_{1i} |\sigma_i|^{1/2} \operatorname{sgn}(\sigma_i) - \omega_{2i} P(\sigma_i) \tag{60}$$

By means of transposing, Eq. (60) changes for

$$\dot{\sigma}_i + \omega_{1i} |\sigma_i|^{1/2} \operatorname{sgn}(\sigma_i) + \omega_{2i} P(\sigma_i) = \bar{D}_i \tag{61}$$

where $\dot{P}(\sigma_i) + T_s P(\sigma_i) = \operatorname{sgn}(\sigma_i)$, $\left|\dot{\bar{D}}_i\right| \le \tilde{g}_i$.

In accordance with Lemma 2, σ_i and $\dot{\sigma}_i$ will converge to zero in finite time, which satisfy $T_{ri} \le 7.6\sigma_i(0)/(\omega_{2i} - \tilde{g}_i)$. It means that

$$\sigma_i = \dot{\sigma}_i = 0 \quad \forall t > T_{ri} \tag{62}$$

Substituting Eq. (62) into Eq. (59), it is obtained that

$$\bar{D}_i = v_i \tag{63}$$

Hence, the disturbance is estimated as

$$\begin{bmatrix} \hat{d}_1(t) \\ \hat{d}_2(t) \end{bmatrix} = \mathbf{B}^{-1} \begin{bmatrix} \bar{D}_1 \\ \bar{D}_2 \end{bmatrix} = \mathbf{B}^{-1} \begin{bmatrix} v_1 \\ v_2 \end{bmatrix} \tag{64}$$

Therefore, the external disturbance can be exactly estimated in finite time. The theorem is proven completely. □

Remark 8 The parameters ω_{1i} and ω_{2i} have a relationship with the disturbance boundary and its derivative boundary $\tilde{g}_i$. So the proposed SMDOB estimates only the bounded disturbance.

Remark 9 The auxiliary sliding mode control variable v_i is continuous due to the discontinuous term sgn (σ_i) is integrated as well as in the presence of the fractional power term $|\sigma_i|^{1/2}$.

On the basis of Theorem 2, the terminal sliding mode controller with SMDOB is designed as

$$u=\begin{bmatrix}\beta_c\\ \delta_e\end{bmatrix}=\mathbf{B}^{-1}\begin{bmatrix}-\Phi_1-F_V+\ddot{V}_d-k_1\,|s_1|^{\gamma_1}\,\mathrm{sgn}(s_1)\\ -\Phi_2-F_h+h_d^{(4)}-k_2\,|s_2|^{\gamma_2}\,\mathrm{sgn}(s_2)\end{bmatrix}-\begin{bmatrix}\hat{d}_1(t)\\ \hat{d}_2(t)\end{bmatrix} \tag{65}$$

Remark 10 The controller of Eq. (65) is improved with respect to the tracking controller of Eq. (30). The former has the rejection for external disturbance.

Remark 11 The chattering phenomenon usually in sliding mode control is significantly reduced, implying the features of recursive terminal sliding mode controller with proposed disturbance observer in Eq. (65). The reason is the sign function item is continuous.

4 Composite controller and stability analysis

In this section, the stability and robustness of the composite controller are analyzed. The composite controller is given in Eq. (65), which consists of RTSMC tracking controller and SMDOB.

Theorem 3 *For the longitudinal dynamics of HFV model* (1)*, the system is stable and robust for the reference command in the presence of parameter uncertainties and external disturbances, if the controller is chosen to Eq.* (65).

Proof Choosing the Lyapunov function candidate $L_a = \frac{1}{2}s^{\mathrm{T}}s$ and taking its time derivative along the sliding mode manifold dynamics in Eq. (51) yields

$$\dot{L}_a = s^{\mathrm{T}}\dot{s} = s^{\mathrm{T}}\left(\begin{bmatrix}F_V-\ddot{V}_d+\Phi_1\\ F_h-h_d^{(4)}+\Phi_2\end{bmatrix}+\mathbf{B}\cdot u+\mathbf{B}\cdot\begin{bmatrix}d_1(t)\\ d_2(t)\end{bmatrix}\right) \tag{66}$$

Substituting Eq. (65) into Eq. (66), the function L_a dynamics is changed as

$$\dot{L}_a = s^{\mathrm{T}}\left(\begin{bmatrix}-k_1\,|s_1|^{\gamma_1}\,\mathrm{sgn}(s_1)\\ -k_2\,|s_2|^{\gamma_2}\,\mathrm{sgn}(s_2)\end{bmatrix}+\mathbf{B}\cdot\begin{bmatrix}\tilde{d}_1(t)\\ \tilde{d}_2(t)\end{bmatrix}\right) \tag{67}$$

where $\tilde{d}_i(t) = d_i(t) - \hat{d}_i(t), i = 1, 2$ is the error between the actual and estimated disturbance.

In accordance with Theorem 2, the external disturbance can be exactly estimated in finite time. The disturbance error $\tilde{d}_i(t)$ will converge to zero in finite time, i.e., $\tilde{d}_i(t) \to 0, \forall t > T_{ri}$. So when $t > T_{ri}$, Eq. (67) is changed as

$$\begin{aligned}\dot{L}_a &= s^{\mathrm{T}}\begin{bmatrix}-k_1\,|s_1|^{\gamma_1}\,\mathrm{sgn}(s_1)\\ -k_2\,|s_2|^{\gamma_2}\,\mathrm{sgn}(s_2)\end{bmatrix}\\ &= -k_1\,|s_1|^{\gamma_1+1}-k_2\,|s_2|^{\gamma_2+1}\le 0\end{aligned} \tag{68}$$

Hence, the sliding mode manifolds s_i $(i = 1, 2)$ equal to zero in finite time, and then, the each layer sliding surface will converge to zero recursively by means of proof process of Theorem 1. Finally, the system can track the reference command. Therefore, the system is stable and robust for uncertainty and disturbance in finite time. This completes the proof. □

Remark 12 In Theorem 3, the finite time is on the basis of $t_i (i = 1, 2)$ in Theorem 1, which also consists of the estimated time for disturbance, namely

$$t_{fi} = t_i + T_{ri}, \quad i = 1, 2 \tag{69}$$

where t_{fi} is the overall time in Theorem 3.

Remark 13 Theorem 3 gives the stability proof from the theory point of view. In the practical engineering, the sampling time may affect the system stability. In order to verify the effect of the sampling time on the convergence of the composed controller (65), simulations with different sampling time are conducted. The results are displayed in Table 1.

It is obviously seen from Table 1 that the sampling time affects the convergence of the system. The shorter the sampling time, the more stable the system. When the sampling time is larger than some value, the system becomes unstable. Therefore, in this paper, the sampling time is selected for 0.001 s.

The structure diagram of composite control scheme for HFV in this paper is shown in Fig. 1.

Table 1 The effect of sampling time on the system

Sampling time (s)	0.0005	0.001	0.002	0.004	0.005	0.007	0.01
Convergence or not (C or N)	C	C	C	C	C	N	N

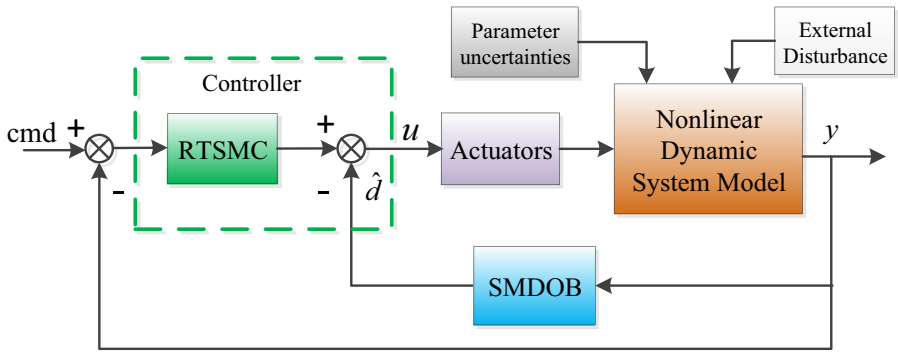

Fig. 1 Structure diagram of composite control scheme

5 Numerical simulations

The numerical simulation of composite controller that comprises RTSMC and SMDOB proposed in previous section is conducted in this section. The simulation is built in the trimmed cruise flight condition of HFV. In the cruise flight condition, the initial simulation parameters are altitude 110,000 ft, velocity 15,060 ft/s, Mach 15, angle of attack 0 rad and pitch rate 0 rad/s, respectively. The damping ratio and natural frequency of the engine dynamics model are taken 0.7 and 5 rad/s, respectively. In the simulation, the reference command for velocity subsystem is step signal 100 ft/s and a step command of 500 ft for altitude subsystem. The nominal dynamic parameters [8] for HFV are presented in Table 2.

The external disturbances in the simulation are selected as

$$d_1(t) = 0.1\sin(0.5t) + 0.15\cos(0.3t) + 0.2\sin(0.6t) \tag{70}$$

$$d_2(t) = 0.2\sin(0.5t) + 0.1\sin(0.3t) + 0.2\cos(0.6t) \tag{71}$$

The disturbances above are added to the system at 70 s in simulation.

Table 2 Nominal dynamic parameters of HFV

Parameter	Value	Unit
m_0	9375	slug
I_0	7×10^6	slug · ft^3
S_0	3603	ft^2
$\bar{c}_0$	80	ft
c_{e0}	0.0292	dimensionless
ρ_0	2.4325×10^{-5}	slug/ft^3

The simulation results of nominal HFV model in the presence of parameter uncertainties controlled by RTSMC tracking controller are shown in Figs. 2 and 3. The results of velocity subsystem are displayed in Figs. 2 and 3 for altitude subsystem.

Figure 2a displays the velocity tracking performance. It is seen from the figure that the aircraft velocity tracks the reference command in about 25 s, and the tracking speed holds constant. Due to the constant speed, the system is influenced when the command is tracked, which can be seen in Fig. 2b–e. The influence of throttle setting β_c is greater in Fig. 2e. But the effects vanish immediately, and the system becomes stable in no time. The other variables also converge to constant value after a limited time in Fig. 2b–e.

The altitude tracking performance is displayed in Fig. 3b. The tracking time to altitude reference command is about 45 s. The tracking speed is not constant in this subsystem. Because the fourth-layer sliding mode manifold is asymptotic convergence, whose speed is not constant. In about 32.5 s, there is a switch from the finite-time convergence sliding surface to the asymptotic convergence sliding surface. So the system is influenced at this time which is obviously seen in Fig. 3a, c–e. Likewise, the effects are small and vanish immediately.

From the Fig. 2d, e and Fig. 3d, e, there is no chattering in the actuators, which verify the stable and robust performances of proposed RTSMC in the presence of parameter uncertainties. The finite-time convergence performance for Theorem 1 is demonstrated in Figs. 2 and 3. The trajectories of sliding variables are shown in Fig. 4.

In Fig. 4a, b are the last-layer sliding manifolds, which are first arrived. Figure 4c, d are the time deriv-

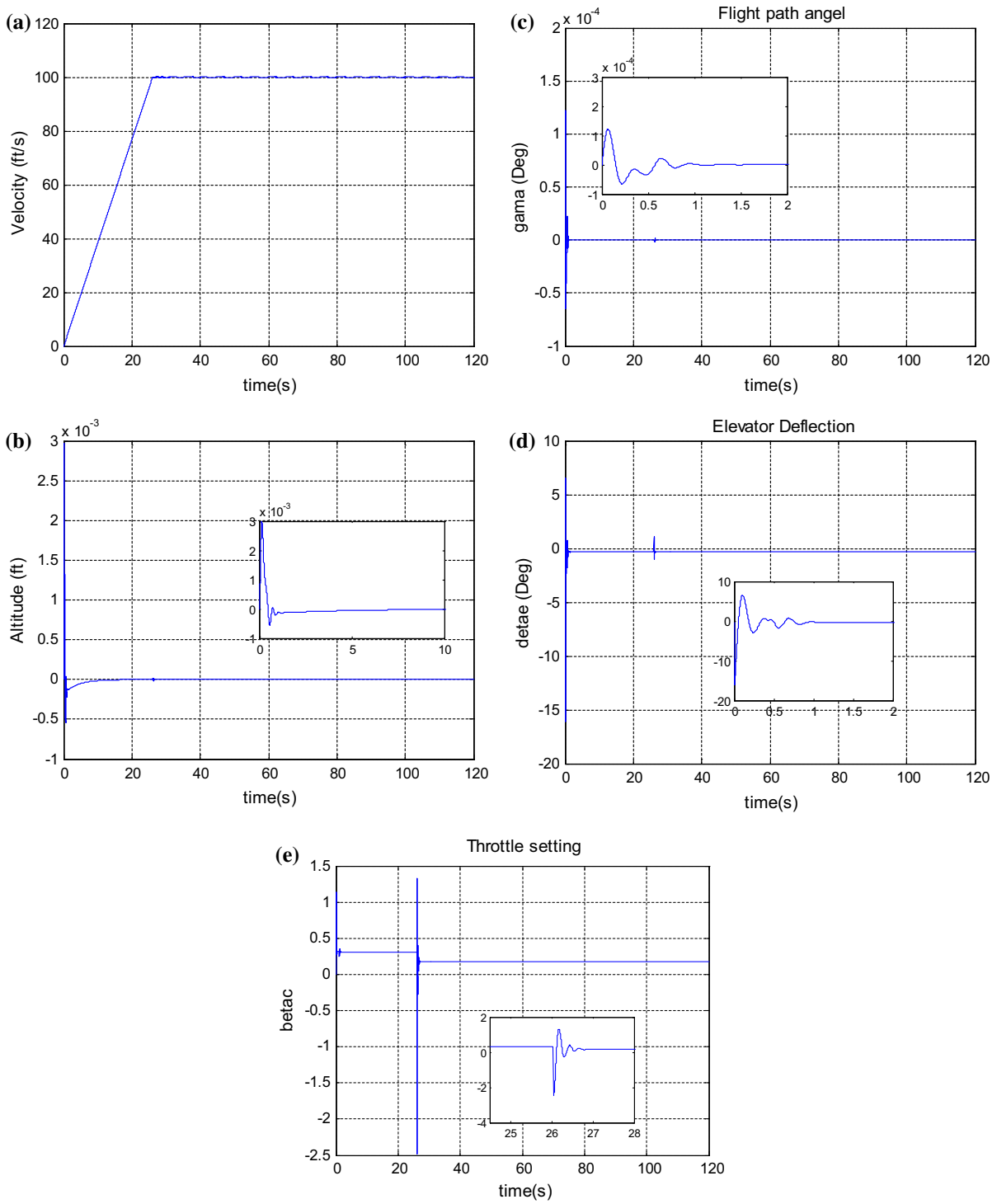

Fig. 2 The velocity subsystem response for nominal model. **a** Velocity, **b** altitude, **c** flight path angle, **d** elevator deflection angle, **e** throttle setting

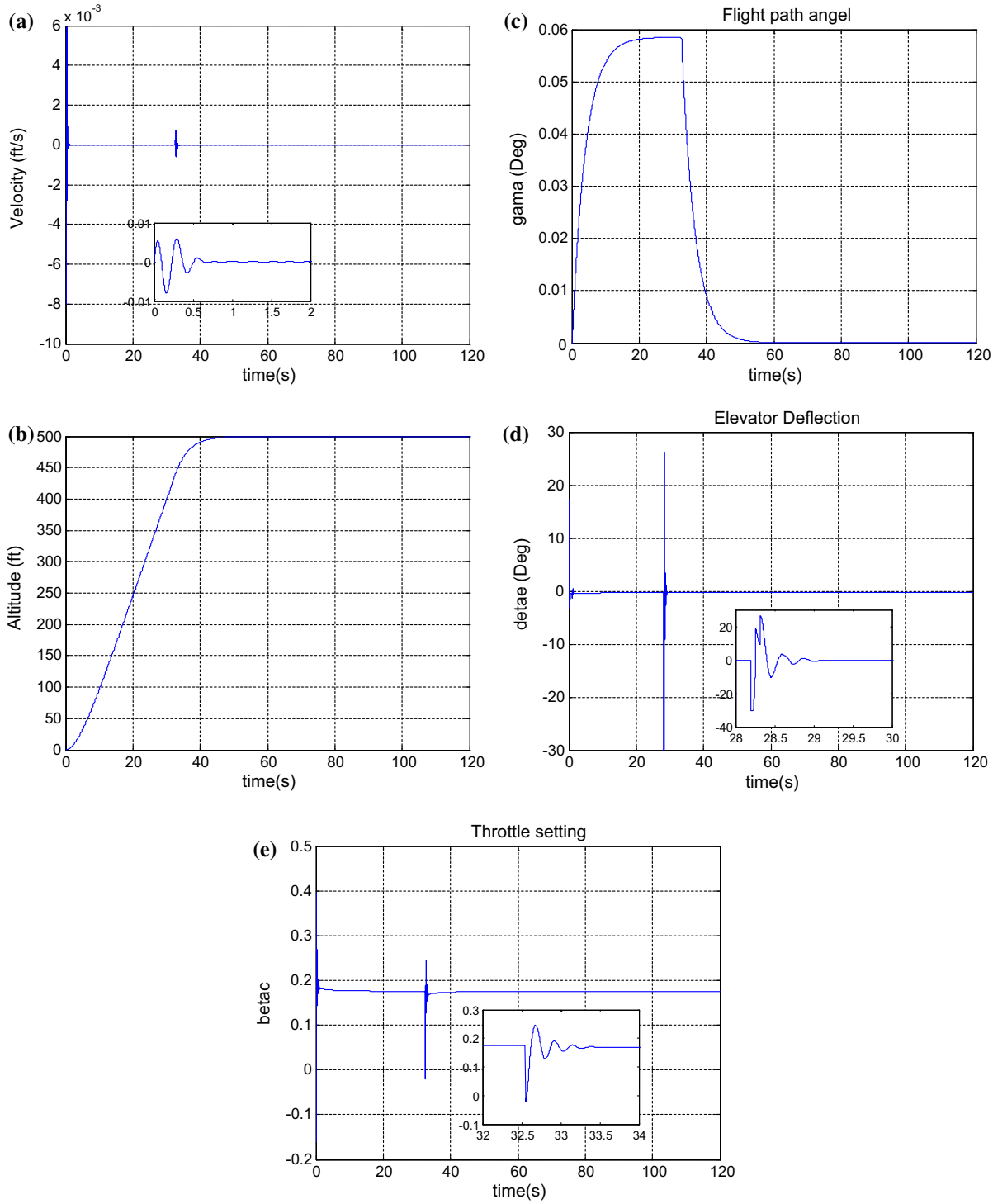

Fig. 3 The altitude subsystem response for nominal model. **a** Velocity, **b** altitude, **c** flight path angle, **d** elevator deflection angle, **e** throttle setting

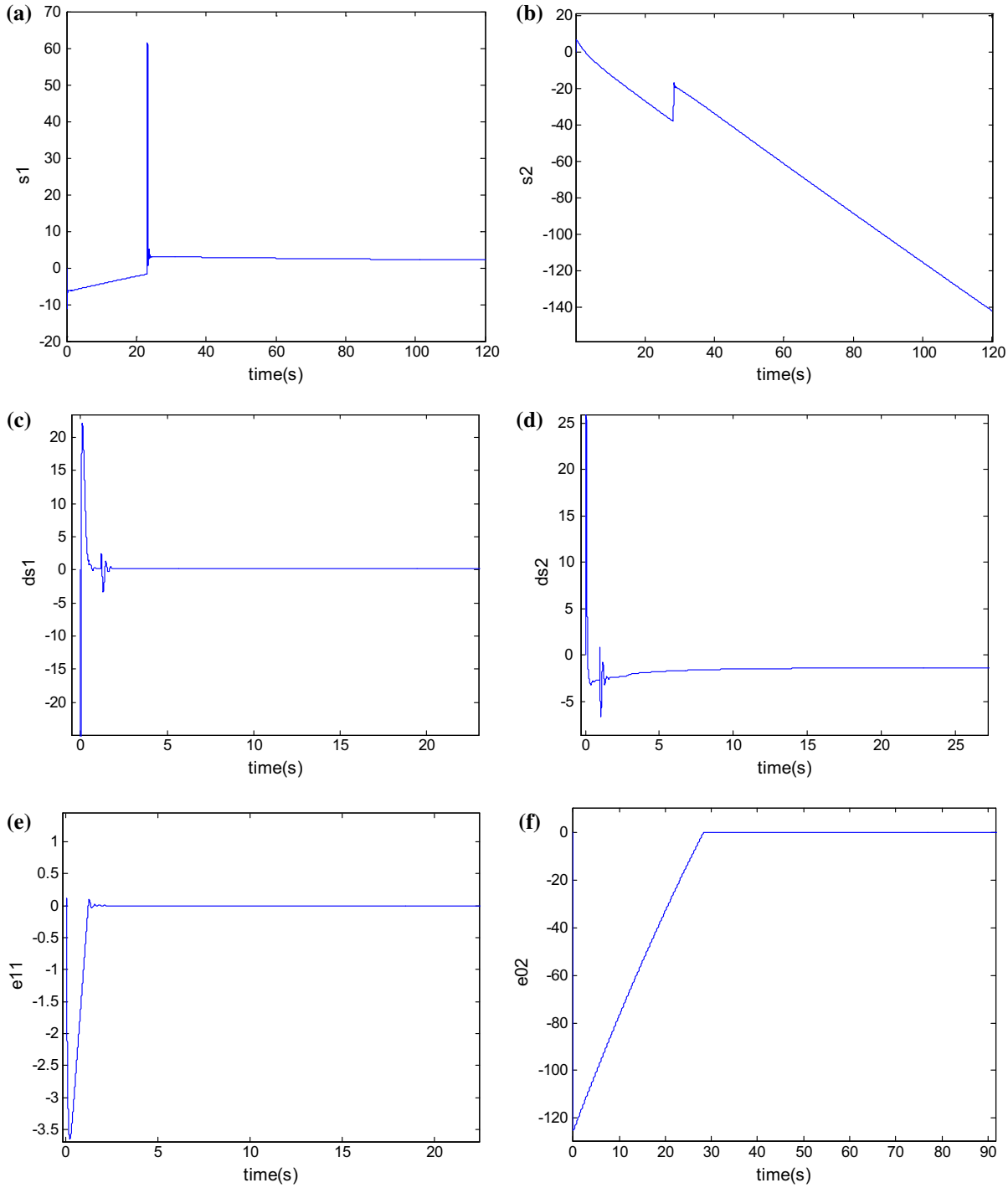

Fig. 4 Trajectories of sliding variables. **a** Variable s_1, **b** variable s_2, **c** variable $\dot{s}_1$, **d** variable $\dot{s}_2$, **e** variable e_{11}, **f** variable e_{02}

atives of variables s_1 and s_2, respectively. Fig. 4e, f are the first-layer sliding mode manifolds, which are related to the system tracking error.

For further demonstrating the validity of the proposed method RTSMC, this method and the traditional SMC in reference [8] which has linear sliding mode

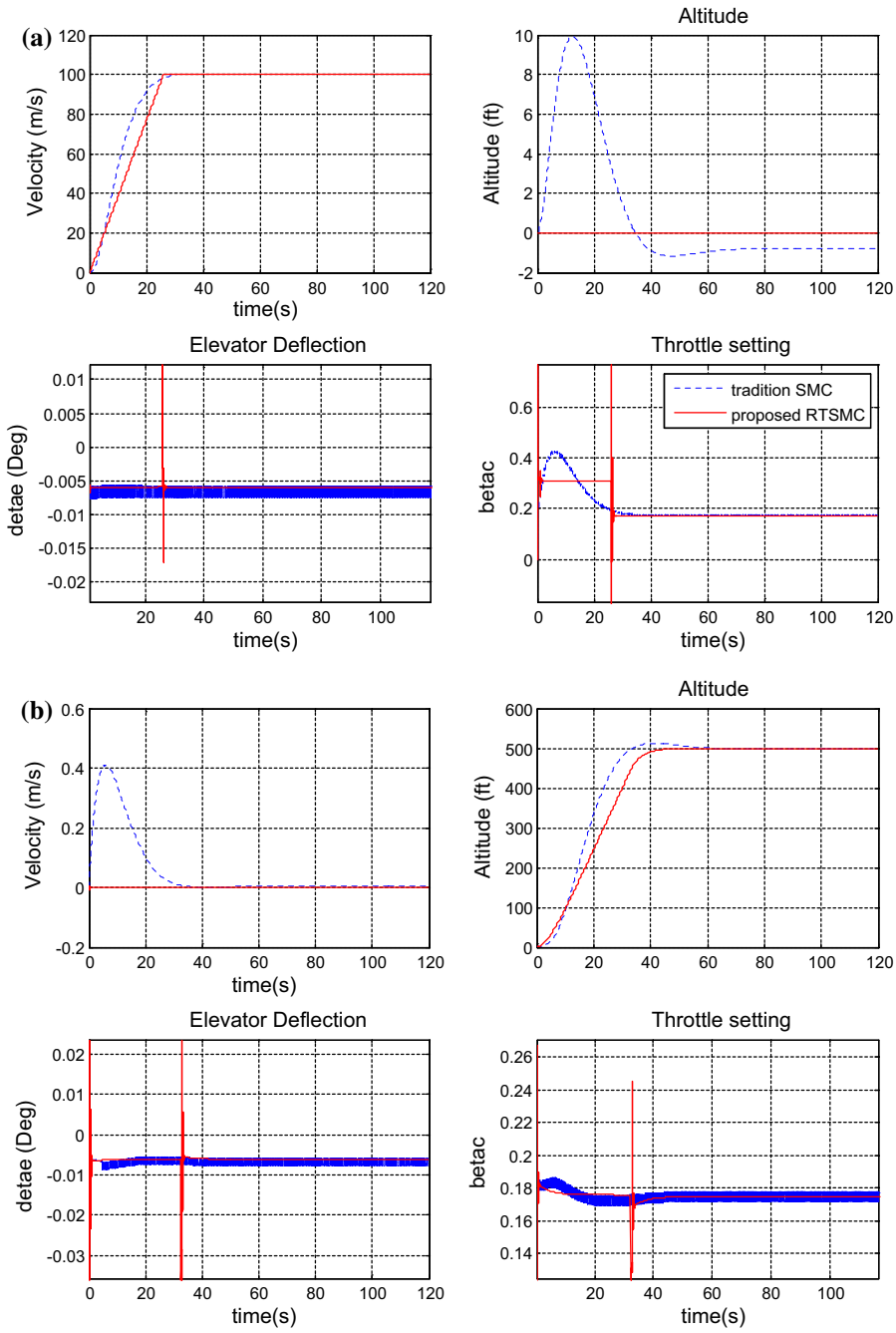

Fig. 5 Comparing results between RTSMC and SMC. **a** Velocity subsystem comparison, **b** altitude subsystem comparison

surfaces are compared for simulation. The simulation results are displayed in Fig. 5.

By the mean of comparison, the convergence time of RTSMC is smaller than that of SMC and the robust of RTSMC is stronger than SMC. The altitude variable in Fig. 5a and velocity variable in Fig. 5b of SMC have larger variation than that of RTSMC. In addition, the actuators for SMC are chattering during the simulation, while the RTSMC are not.

When the external disturbances in Eqs. (70) and (71) are considered, the simulation results controlled by RTSMC are shown in Figs. 6 and 7.

From Figs. 6 to 7, the system responses are impacted by external disturbances after 70 s. Comparing Fig. 2

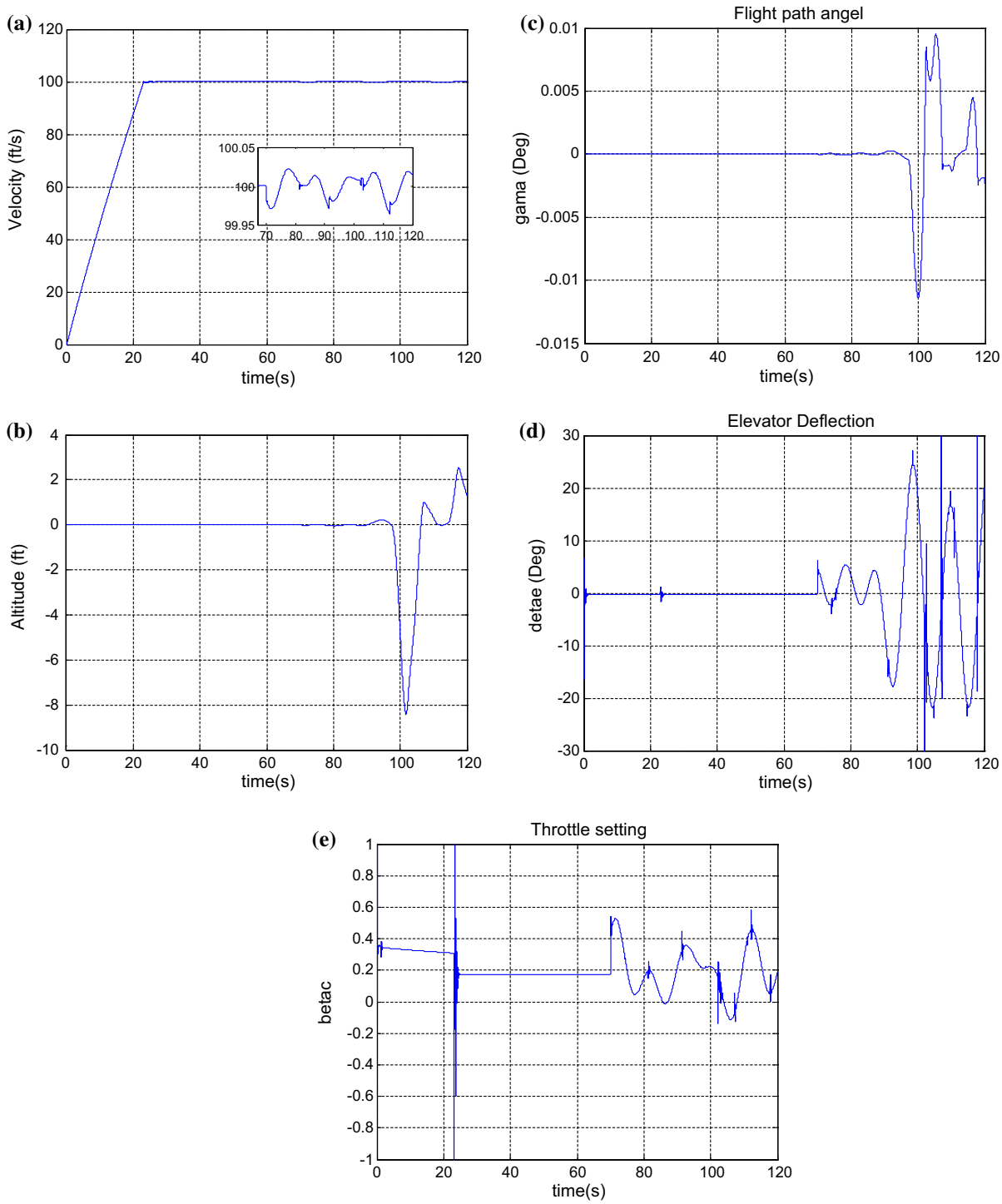

Fig. 6 The velocity subsystem response for disturbance. **a** Velocity, **b** altitude, **c** flight path angle, **d** elevator deflection angle, **e** throttle setting

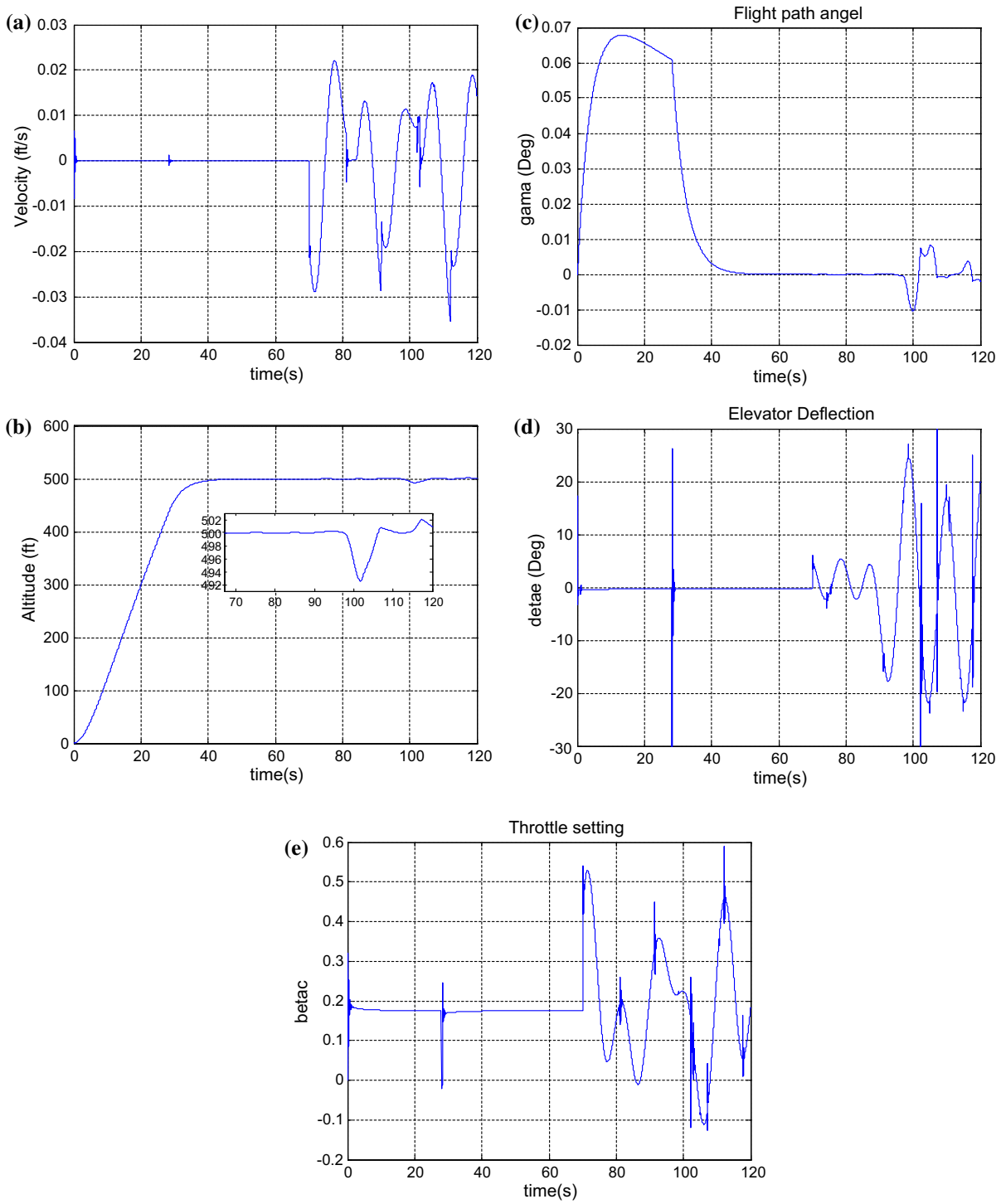

Fig. 7 The altitude subsystem response for disturbance. **a** Velocity, **b** altitude, **c** flight path angle, **d** elevator deflection angle, **e** throttle setting

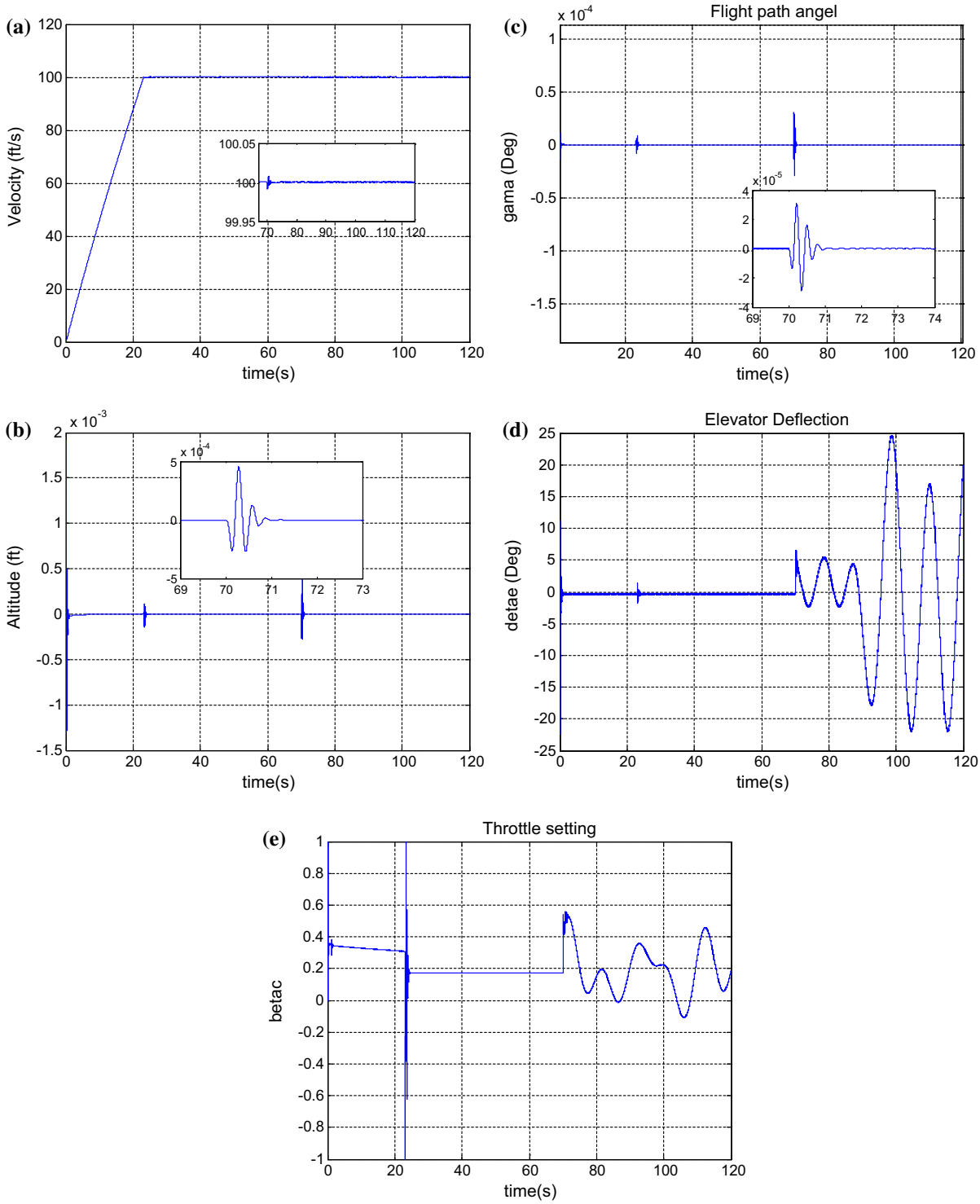

Fig. 8 The velocity subsystem response with SMDOB. **a** Velocity, **b** altitude, **c** flight path angle, **d** elevator deflection angle, **e** throttle setting

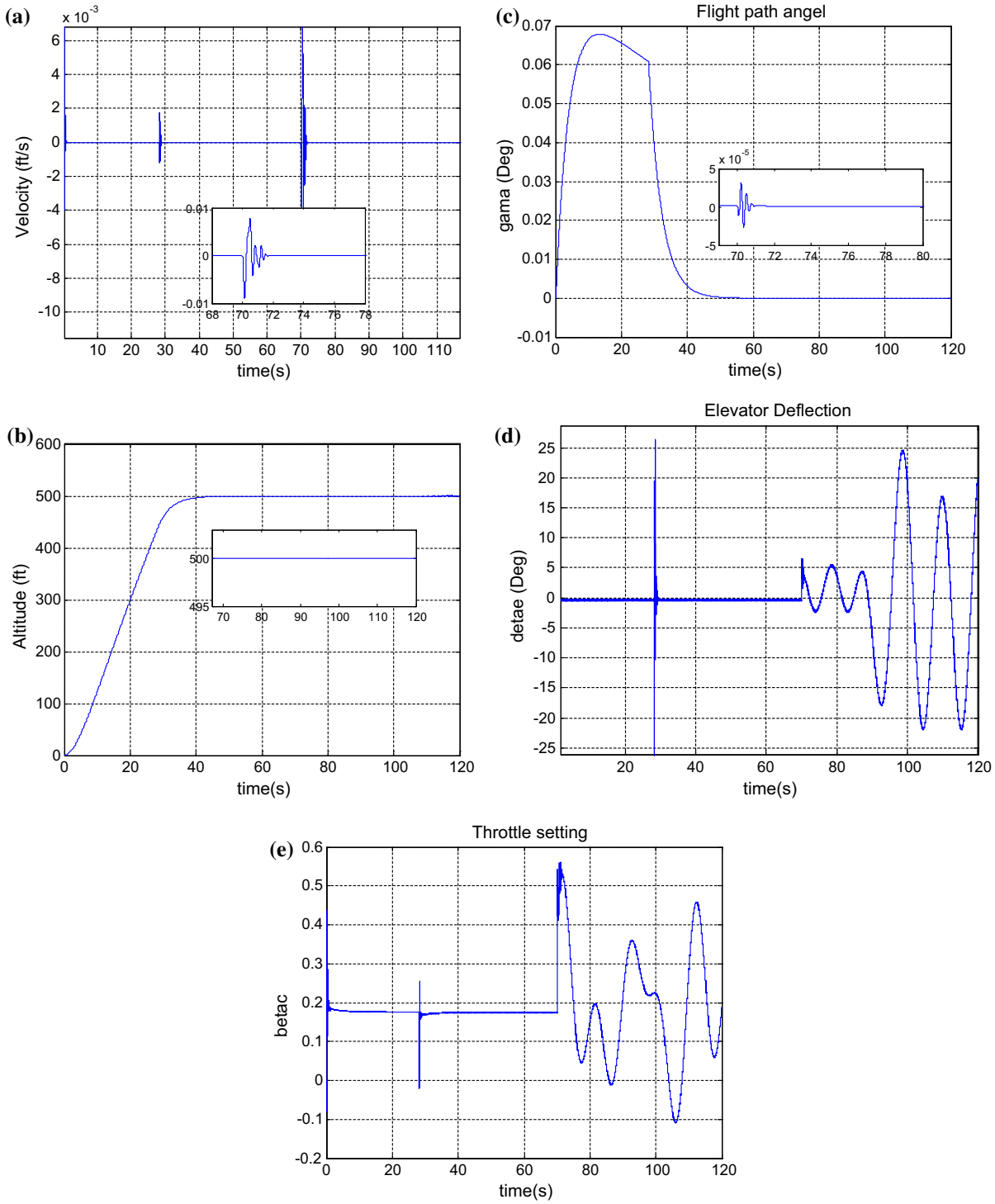

Fig. 9 The altitude subsystem response with SMDOB. **a** Velocity, **b** altitude, **c** flight path angle, **d** elevator deflection angle, **e** throttle setting

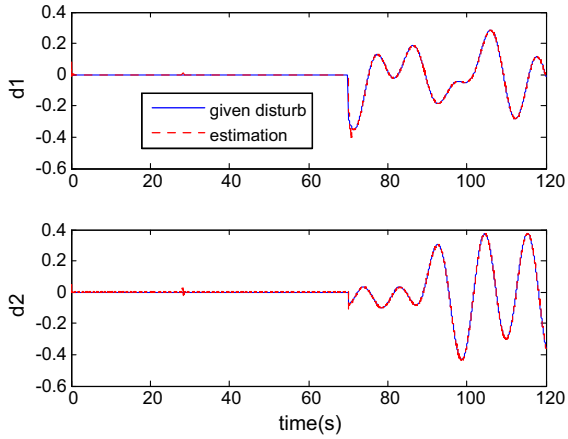

Fig. 10 The external disturbance and its estimation by SMDOB

and 6, Fig. 3 and 7, the stable and tracking performances of the system are not affected before adding into the external disturbances.

When the proposed SMDOB is implied to estimate the disturbance and compensate the controller, the system responses are shown in Figs. 8 and 9.

Comparing Figs. 6a–c and 8a–c, Fig. 7a–c and 9a–c, respectively, it is obviously seen that perfect performance is obtained for SMDOB. The disturbance in velocity V, altitude h, flight path angle γ is eliminated by SMDOB, which is reflected in Figs. 8a–c and 9a–c. The external disturbance is estimated by SMDOB, and then, it is compensated in the controller, which is revealed in Figs. 8d, e and 9d, e. The estimation for external disturbance is shown in Fig. 10.

The external disturbance is well estimated by SMDOB from Fig. 10. This implies that the method of SMDOB is valid and available.

In order to verify the influence of measurement noises on the composed controller (65), some random noises are added in the system. Then, the simulation results with random noises are shown in Fig. 11.

In Fig. 11, the system output variables are convergent in spite of having small deviation. So the measurement noises do not affect the convergence of the composed controller, which demonstrates the strong robustness of the proposed controller.

In terms of above simulation, the perfect tracking and disturbance rejection performance are obtained for the longitudinal dynamic system of HFV controlled by RTSMC with SMDOB. The proposed method is stable in finite time. With the method, the system is robust with respect to parameter uncertainties and random noises and the chattering is eliminated in actuator. The external disturbance is estimated in finite time through SMDOB, which has high-precision estimation.

6 Conclusions

The recursive terminal sliding mode controller with sliding mode disturbance observer for longitudinal dynamics of generic hypersonic flight vehicle is proposed in this paper. First, a recursive terminal sliding mode tracking controller is designed by means of recursive terminal sliding mode theory. This controller is finite-time convergence and robust for parameter uncertainties. Next, a sliding mode disturbance observer is

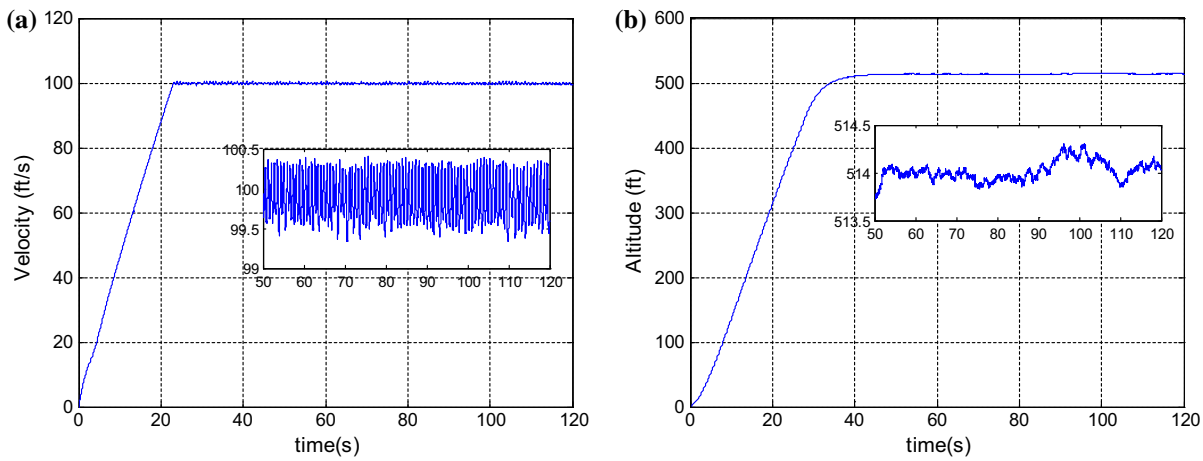

Fig. 11 Simulation results with measurement noises. **a** Velocity, **b** altitude

designed for external disturbance, whose estimation process is also finite time. Then, the composite controller embracing above tracking controller and disturbance observer is suggested. Finally, the numerical simulation for trimmed cruise flight condition of hypersonic flight vehicle is conducted. The simulation results show that the proposed scheme satisfies the expected performance.

Acknowledgments This work was supported by the National Natural Science Foundation of China (91216304).

Appendix 1

The detailed expressions of the vectors $\boldsymbol{\Omega}_1$, $\boldsymbol{\Pi}_1$ and matrices $\boldsymbol{\Omega}_2$, $\boldsymbol{\Pi}_2$ are as follows:

$$\boldsymbol{\Omega}_1 = \begin{bmatrix} \left(\frac{\partial T}{\partial V}\right)\cos\alpha - \frac{\partial D}{\partial V} \\ -\frac{m\mu\cos\gamma}{r^2} \\ -T\sin\alpha - \left(\frac{\partial D}{\partial \alpha}\right) \\ \left(\frac{\partial T}{\partial \beta}\right)\cos\alpha \\ \frac{2m\mu\sin\gamma}{r^3} \end{bmatrix}^{\mathrm{T}}$$

$$\boldsymbol{\Omega}_2 = \begin{bmatrix} \boldsymbol{\omega}_{21} & \boldsymbol{\omega}_{22} & \boldsymbol{\omega}_{23} & \boldsymbol{\omega}_{24} & \boldsymbol{\omega}_{25} \end{bmatrix}$$

where

$$\boldsymbol{\omega}_{21} = \begin{bmatrix} \left(\frac{\partial^2 T}{\partial V^2}\right)\cos\alpha - \frac{\partial^2 D}{\partial V^2} \\ 0 \\ -\left(\frac{\partial T}{\partial V}\right)\sin\alpha - \frac{\partial^2 D}{\partial V\partial\alpha} \\ \left(\frac{\partial^2 T}{\partial V\partial\beta}\right)\cos\alpha \\ 0 \end{bmatrix}, \boldsymbol{\omega}_{22} = \begin{bmatrix} 0 \\ \frac{m\mu\sin\gamma}{r^2} \\ 0 \\ 0 \\ \frac{2m\mu\cos\gamma}{r^3} \end{bmatrix},$$

$$\boldsymbol{\omega}_{23} = \begin{bmatrix} -\left(\frac{\partial T}{\partial V}\right)\sin\alpha - \left(\frac{\partial^2 D}{\partial V\partial\alpha}\right) \\ 0 \\ -T\cos\alpha - \left(\frac{\partial^2 D}{\partial\alpha^2}\right) \\ -\left(\frac{\partial T}{\partial\beta}\right)\sin\alpha \\ 0 \end{bmatrix}$$

$$\boldsymbol{\omega}_{24} = \begin{bmatrix} \frac{\partial^2 T}{\partial V\partial\beta}\cos\alpha \\ 0 \\ -\left(\frac{\partial T}{\partial\beta}\right)\sin\alpha \\ 0 \\ 0 \end{bmatrix}, \boldsymbol{\omega}_{25} = \begin{bmatrix} 0 \\ \frac{2m\mu\cos\gamma}{r^3} \\ 0 \\ 0 \\ -\frac{6m\mu\sin\gamma}{r^4} \end{bmatrix}$$

$$\boldsymbol{\Pi}_1 = \begin{bmatrix} \frac{\partial L/\partial V + (\partial T/\partial V)\sin\alpha}{mV} - \frac{L+T\sin\alpha}{mV^2} + \frac{\mu\cos\gamma}{V^2r^2} + \frac{\cos\gamma}{r} \\ \frac{\mu\sin\gamma}{Vr^2} - \frac{V\sin\gamma}{r} \\ \frac{\partial L/\partial\alpha + T\cos\alpha}{mV} \\ \frac{(\partial T/\partial\beta)\sin\alpha}{mV} \\ \frac{2\mu\cos\gamma}{Vr^3} - \frac{V\cos\gamma}{r^2} \end{bmatrix}^{\mathrm{T}}$$

$$\boldsymbol{\Pi}_2 = \begin{bmatrix} \boldsymbol{\pi}_{21} & \boldsymbol{\pi}_{22} & \boldsymbol{\pi}_{23} & \boldsymbol{\pi}_{24} & \boldsymbol{\pi}_{25} \end{bmatrix}$$

$$\boldsymbol{\pi}_{21} = \begin{bmatrix} \frac{\partial^2 L/\partial V^2 + (\partial^2 T/\partial V^2)\sin\alpha}{mV} - \frac{2[\partial L/\partial V + (\partial T/\partial V)\sin\alpha]}{mV^2} \\ +\frac{2(L+T\sin\alpha)}{mV^3} - \frac{2\mu\cos\gamma}{V^3r^2} - \frac{\mu\sin\gamma}{V^2r^2} - \frac{\sin\gamma}{r} \\ \frac{(\partial^2 L/\partial\alpha\partial V) + (\partial T/\partial V)\cos\alpha}{mV} - \frac{\partial L/\partial\alpha + T\cos\alpha}{mV^2} \\ \frac{(\partial^2 T/\partial\beta\partial V)\sin\alpha}{mV} - \frac{(\partial T/\partial\beta)\sin\alpha}{mV^2} \\ -\frac{2\mu\cos\gamma}{V^2r^3} - \frac{\cos\gamma}{r^2} \end{bmatrix}$$

$$\boldsymbol{\pi}_{22} = \begin{bmatrix} -\frac{\mu\sin\gamma}{V^2r^2} - \frac{\sin\gamma}{r} \\ \frac{\mu\cos\gamma}{Vr^2} - \frac{V\cos\gamma}{r} \\ 0 \\ 0 \\ -\frac{2\mu\sin\gamma}{Vr^3} + \frac{V\sin\gamma}{r^2} \end{bmatrix},$$

$$\boldsymbol{\pi}_{23} = \begin{bmatrix} \frac{(\partial^2 L/\partial V\partial\alpha) + (\partial T/\partial V)\cos\alpha}{mV} - \frac{\partial L/\partial\alpha + T\cos\alpha}{mV^2} \\ 0 \\ \frac{\partial^2 L/\partial\alpha^2 - T\sin\alpha}{mV} \\ \frac{(\partial T/\partial\beta)\cos\alpha}{mV} \\ 0 \end{bmatrix}$$

$$\boldsymbol{\pi}_{24} = \begin{bmatrix} \frac{(\partial^2 T/\partial V\partial\beta)\sin\alpha}{mV} - \frac{(\partial T/\partial\beta)\sin\alpha}{mV^2} \\ 0 \\ \frac{(\partial T/\partial\beta)\cos\alpha}{mV} \\ 0 \\ 0 \end{bmatrix},$$

$$\boldsymbol{\pi}_{25} = \begin{bmatrix} -\frac{2\mu\cos\gamma}{V^2r^3} - \frac{\cos\gamma}{r^2} \\ -\frac{2\mu\sin\gamma}{Vr^3} + \frac{V\sin\gamma}{r^2} \\ 0 \\ 0 \\ -\frac{6\mu\cos\gamma}{Vr^4} + \frac{2V\cos\gamma}{r^3} \end{bmatrix}$$

Appendix 2

Without loss of generality, the angle of attack and flight path angle are assumed near this singularity to be

$$\alpha = \varepsilon, \gamma = \frac{\pi}{2} \tag{72}$$

where ε is a small positive number.

Then,

$$\begin{aligned} b_{11} &= \left(\frac{\rho V^2 S c_\beta \omega_n^2}{2m}\right)\cos\alpha = \left(\frac{\rho V^2 S c_\beta \omega_n^2}{2m}\right)\cos\varepsilon \\ &\approx \frac{\rho V^2 S c_\beta \omega_n^2}{2m} \end{aligned} \tag{73}$$

$$b_{12} = -\left(\frac{c_e \rho V^2 S\bar{c}}{2mI_{yy}}\right)(T\sin\alpha + D_\alpha)$$

$$\approx -\left(\frac{c_e \rho V^2 S\bar{c}}{2mI_{yy}}\right)(T\varepsilon + \sigma) \tag{74}$$

where $\sigma = \frac{\partial\left(\frac{1}{2}\rho V^2 S C_D\right)}{\partial\alpha}$ and which is a small real number.

$$\begin{aligned} b_{21} &= \left(\frac{\rho V^2 S c_\beta \omega_n^2}{2m}\right)\sin(\alpha+\gamma) \\ &= \left(\frac{\rho V^2 S c_\beta \omega_n^2}{2m}\right)\sin(\varepsilon+\frac{\pi}{2}) \approx \frac{\rho V^2 S c_\beta \omega_n^2}{2m} \end{aligned} \tag{75}$$

$$\begin{aligned} b_{22} &= \left(\frac{c_e \rho V^2 S\bar{c}}{2mI_{yy}}\right)\left[T\cos(\alpha+\gamma)\right. \\ &\quad \left. + L_\alpha \cos\gamma - D_\alpha \sin\gamma\right] \\ &\approx \left(\frac{c_e \rho V^2 S\bar{c}}{2mI_{yy}}\right)(0+0-\sigma) \\ &= -\sigma\left(\frac{c_e \rho V^2 S\bar{c}}{2mI_{yy}}\right) \end{aligned} \tag{76}$$

In the above case, b_{11} is equal to b_{21}, and the matrix $\mathbf{B}$ will be singular if $b_{12} = b_{22} = 0$. Therefore, we give b_{12} and b_{22} some restrictions near the singularity, namely

$$b_{12} = \begin{cases} \delta_1^*, |b_{12}| \le \delta_1^* \\ b_{12}, |b_{12}| > \delta_1^* \end{cases} \tag{77}$$

$$b_{22} = \begin{cases} \delta_2^*, |b_{22}| \le \delta_2^* \\ b_{22}, |b_{22}| > \delta_2^* \end{cases} \tag{78}$$

moreover, $\delta_1^* \neq \delta_2^*$, $b_{12} \neq b_{22}$.

In that way, the matrix

$$\mathbf{B} = \begin{bmatrix} b_{11} & b_{12} \\ b_{21} & b_{22} \end{bmatrix} \neq \mathbf{0} \tag{79}$$

And the controller in the paper can be used.

References

1. Chavez, F.R., Schmidt, D.K.: Analytical aeropropulsive/aeroelastic hypersonic vehicle model with dynamic analysis. J. Guid. Control Dyn. **17**(6), 1308–1319 (1994)
2. Bolender, M.A., Doman, D.B.: A non-linear model for the longitudinal dynamics of a hypersonic air-breathing vehicle. Defense Technical Information Center (2006)
3. Bolender, M.A., Doman, D.B.: Nonlinear longitudinal dynamical model of an air-breathing hypersonic vehicle. J Spacecr. Rockets **44**(2), 374–387 (2007)
4. Marrison, C.I., Stengel, R.F.: Design of robust control systems for hypersonic aircraft. J. Guid. Control Dyn. **21**(1), 58–63 (1998)
5. Wang, Q., Stengel, R.F.: Robust nonlinear control of a hypersonic aircraft. J. Guid. Control Dyn. **23**(4), 577–585 (2000)
6. Groves, K.P., Sigthorsson, D.O., Serrani, A., Yurkovich, S.: Reference command tracking for a linearized model of an air-breathing hypersonic vehicle. In: AIAA Guidance, Navigation, and Control Conference and Exhibit, San Francisco, CA (2005)
7. Parker, J.T., Bolender, M.A., Doman, D.B.: Control-oriented modeling of an air-breathing hypersonic vehicle. J. Guid. Control Dyn. **30**(3), 856–869 (2007)
8. Xu, H., Mirmirani, M.D., Ioannou, P.A.: Adaptive sliding mode control design for a hypersonic flight vehicle. J. Guid. Control Dyn **27**(5), 829–838 (2004)
9. Rehman, O.U., Fidan, B., Petersen, I.R.: Uncertainty modeling and robust minimax LQR control of multivariable nonlinear systems with application to hypersonic flight. Asian J. Control **14**(5), 1180–1193 (2012)
10. Rehman, O.U., Petersen, I.R., Fidan, B.: Robust nonlinear control design of a hypersonic flight vehicle using minimax linear quadratic Gaussian control. In: 49th IEEE Conference on Decision and Control, Atlanta, GA, USA, pp 6219–6224 (2010)
11. Rehman, O.U., Petersen, I.R., Fidan, B.: Feedback linearization-based robust nonlinear control design for hypersonic flight vehicles. Proc. IMechE Part I: J Syst. Control Eng. **227**(1), 3–11 (2012)
12. Hu, X., Karimi, H.R., Zhang, Z., Gao, H.: Non-fragile sliding mode control for flexible air-breathing hypersonic vehicles. In: 7th IEEE Conference on Industrial Electronics and Applications (ICIEA), Singapore, pp. 906–911 (2012)
13. Durmaz, B., Özgören, M.K., Salamci, M.U.: Sliding mode control for non-linear systems with adaptive sliding surfaces. Trans. Inst. Meas. Control **34**(1), 56–90 (2012)
14. Hu, X., Wu, L., Hu, C., Gao, H.: Adaptive sliding mode tracking control for a flexible air-breathing hypersonic vehicle. J. Franklin Inst. **349**, 559–577 (2012)
15. Yu, X., Zhihong, M.: Fast terminal sliding-mode control design for nonlinear dynamical systems. IEEE Trans. Circuits Syst. I Fundam. Theory Appl. **49**(2), 261–264 (2002)
16. Yu, S., Yu, X., Shirinzadeh, B., Man, Z.: Continuous finite-time control for robotic manipulators with terminal sliding mode. Automatica **41**, 1957–1964 (2005)
17. Feng, Y., Yu, X., Man, Z.: Non-singular terminal sliding mode control of rigid manipulators. Automatica **38**, 2159–2167 (2002)
18. Li, H., Dou, L., Zhong, S.: Adaptive nonsingular fast terminal sliding mode control for electromechanical actuator. Int. J. Syst. Sci. **44**(3), 401–415 (2013)
19. Zhang, R., Sun, C., Zhang, J., Zhou, Y.: Second-order terminal sliding mode control for hypersonic vehicle in cruising flight with sliding mode disturbance observer. J. Control Theory Appl. **11**(2), 299–305 (2013)
20. Zong, Q., Wang, J., Tian, B., Tao, Y.: Quasi-continuous high-order sliding mode controller and observer design for flexible hypersonic vehicle. Aerosp. Sci. Technol. **27**, 127–137 (2013)
21. Sun, H., Li, S., Sun, C.: Finite time integral sliding mode control of hypersonic vehicles. Nonlinear Dyn. **73**, 229–244 (2013)
22. Wilcox, Z.D., MacKunis, W., Bhat, S., Lind, R., Dixon, W.E.: Lyapunov-based exponential tracking control of a hypersonic aircraft with aerothermoelastic effects. J. Guid. Control Dyn. **33**(4), 1213–1224 (2010)

23. Slotine, J.-J.E., Li, W.: Applied Nonlined Control. Pearson Education Inc, New York (1991)
24. Hu, S.: Automatic Control Theory. Science Press, Beijing (2000). (in Chinese)
25. Polyakov, A., Poznyak, A.: Reaching time estimation for "Super-Twisting" second order sliding mode controller via Lyapunov function designing. IEEE Trans. Autom. Control **54**(8), 1951–1955 (2009)
26. Chiu, C.-S.: Derivative and integral terminal sliding mode control for a class of MIMO nonlinear systems. Automatica **48**, 316–326 (2012)
27. Hall, C.E., Shtessel, Y.B.: Sliding mode disturbance observer-based control for a reusable launch vehicle. J. Guid. Control Dyn. **29**(6), 1315–1328 (2006)